Nb surface morphology as a template for heteroepitaxial stacking

LETTER TO THE EDITOR

Nb surface morphology as a template for heteroepitaxial stacking

G L Zhou†, S Bonham‡ and C P Flynn‡

† Materials Science and Engineering Department and Materials Research Laboratory, University of Illinois at Urbana-Champaign, Urbana, IL 61801, USA
‡ Physics Department and Materials Research Laboratory, University of Illinois at Urbana-Champaign, Urbana, IL 61801, USA

Abstract.   We report mesoscopic surface morphologies that occur on Nb surfaces during normal epitaxial growth on miscut sapphire. These features are remarkably effective as growth templates which give selectivity up to approximately $10^3 : 1$ between the two alternative stacking sequences of fcc metals, when grown heteroepitaxially on Nb.

Materials of technical interest and materials of scientific value are both commonly synthesized as thin film single crystals using heteroepitaxy. New control parameters that permit the design and assembly of desired epitaxial structures are therefore much sought. In the synthesis of metallic films by heteroepitaxy, the most widely employed pathways start from semiconductors [1] and from sapphire buffered with a refractory metal, commonly bcc [2, 3], but with fcc and hcp alternatives available [4]. For heteroepitaxy on sapphire, of concern here, the combination Al_2O_3/bcc (e.g. Nb) has special attraction because different available cuts of epitaxial grade Al_2O_3 give high-quality Nb in different orientations [2, 3], and hence direct access to a variety of template symmetries. Over recent years this has furthered the epitaxial growth of tailored single-crystal transition metals and their compounds and alloys [5–7]. In addition it has permitted the growth of more exotic materials such as rare earth nanostructures [8, 9], of compounds and intermetallics with up to 80 atoms per unit cell [10], and a variety of other useful materials. The present paper reports two discoveries that relate directly to the Al_2O_3/Nb pathway. First, we find that Nb grown this way exhibits mesoscopic morphologies which depend sensitively on the growth conditions. Strain-induced mesostructures have recently been of great interest in the epitaxial growth of semiconductors [11–13]. Second, these same Nb mesoscopic structures act as templates which select particular structural features in subsequent heteroepitaxial growth. As an example we describe here the enhancement by a factor of $\sim 10^3$ of ABC stacking relative to ACB stacking in the growth of an fcc (111) metal or, more specifically, Cu_3Au in the $L1_2$ structure.

   In this work, Nb was grown on carefully prepared sapphire substrates by methods of molecular beam epitaxy (MBE) detailed elsewhere [2]. Care was taken to verify that none of the morphologies described here was influenced by residual vacuum gases. Figure 1 shows atomic force microscope (AFM) images of Nb grown ~ 1000 Å thick at temperatures from $700\,°C$ to $1000\,°C$. The rms roughnesses given in the caption are greatest for the $900\,°C$ sample. Also shown is the dependence on the size and orientation of vicinal miscut for those crystals grown at $900\,°C$.
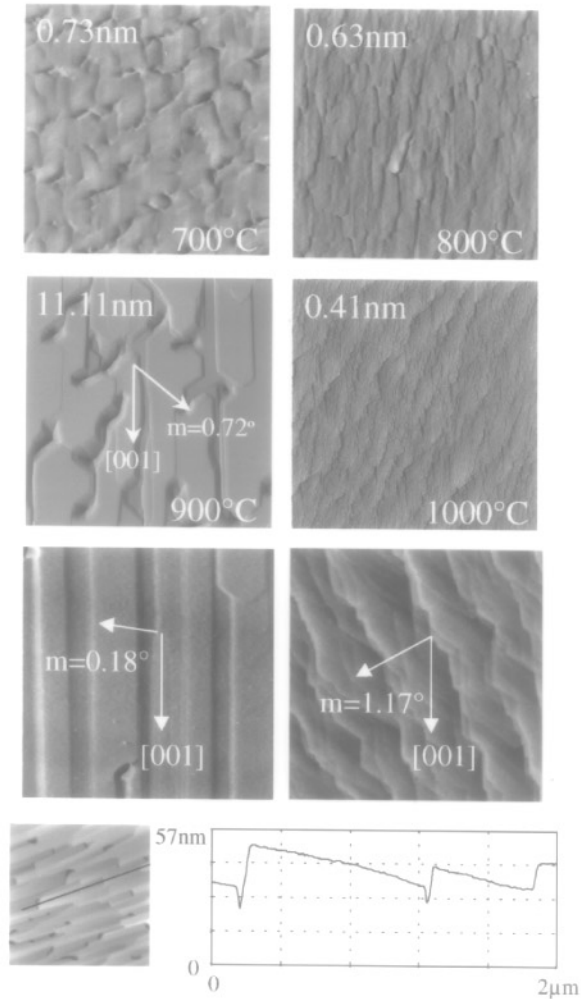
Figure 1. AFM micrographs showing surface features of 1000 Å thick Nb films grown at various temperatures (upper four images) on a sapphire substrate with a miscut $m = 0.72°$. All the images were taken with the same scale, $2 \times 2 \ \mu m^2$ in size. The rms roughness is indicated in the upper left corners. The dependence on miscut m at $T = 900 °C$ is further shown for three images. At the bottom is shown the surface profile for the line drawn along the fingers (bcc [001] axis) in the image reproduced at the lower left. The sample is grown 500 Å thick at 900 °C on a sapphire with a miscut about 0.7° along the finger direction.

Of particular interest here is the mesoscopic fingered structure apparent in the 900 °C crystals, with the long axis of the fingers generally along Nb [001] and ⟨111⟩-type steps at the ends. The height profile along the line in the figure at the bottom left has a remarkable sawtooth form, as shown below the AFM images. The tilt corresponds to that of the sapphire surface, which is miscut from (110) by about 0.7° along the [001] scan. The gentle slope of the sawtooth and the steep escarpment are both Nb {110}-type planes, which evolve during growth by a faceting process. The facets that end the fingers are also {110}-type, ending in the ⟨111⟩ step edges apparent in figure 1. We find that different miscuts give rise to varied
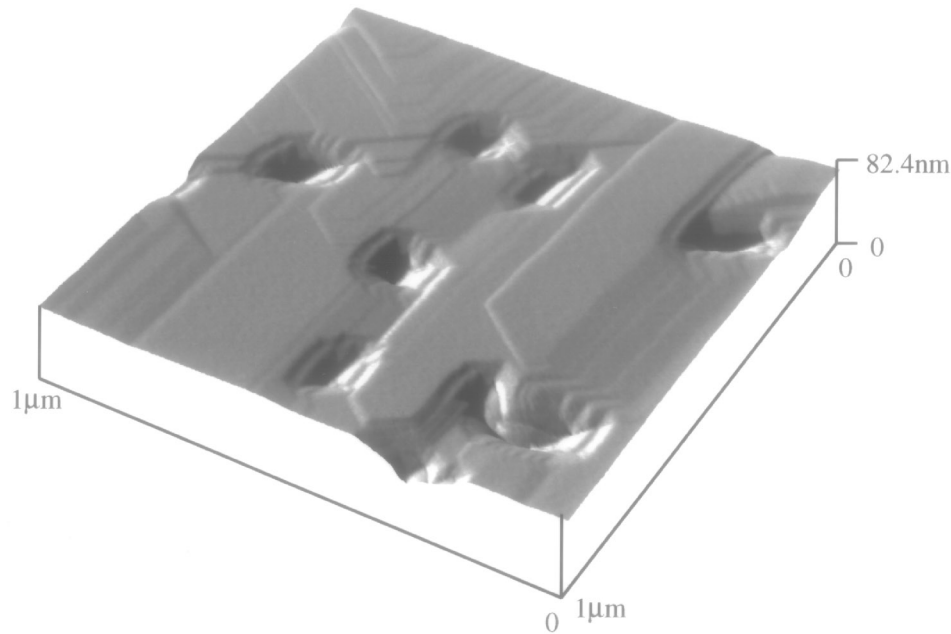
Figure 2. AFM showing 3D topography and the relationship between the ledges and the pinholes for a fingered sample grown 500 Å thick at $1000\,^{\circ}$C on a substrate miscut along [$\bar{1}11$] by about 0.7°.

morphologies, but a temperature regime of analogously faceted morphology always occurs for a miscut of $\geqslant 0.3^{\circ}$. It is eventually covered as the film grows thicker and smoother.

We observe that the fingering and the pinholes visible in figure 1 occur when the tilted mesas of separate islands grow together. An image from a different fingered sample, given in figure 2, shows how ledges of the outer surface continue into the sides of the pinholes. This sample was grown 500 Å thick at $1000\,^{\circ}$C on a substrate miscut along [$\bar{1}11$] by about 0.7°. Further study shows that misfit strain plays a significant role in the evolution of morphology. These processes will be documented more fully in a complete report [14].

Nb makes an excellent non-reactive template for subsequent heteroepitaxial growth. Following electron diffraction studies [7] of the order–disorder phase transition on the (111) surface of Cu_3Au grown on Nb(110), with the Nb itself deposited on the fingering regime near $900\,^{\circ}$C, we have had occasion to further examine the detailed structure of the films, using x-ray diffraction. The structure these diffraction patterns reveal is the second main point of this letter. In this research the Cu_3Au was grown at about $320\,^{\circ}$C where the equilibrium phase diagram shows that the fcc high-temperature phase has developed the superlattice order of the L_{12} structure, in which Au atoms occupy corner sites of the fcc cube. In practice, we observe that epitaxial growth creates, instead, the high-temperature *dis*ordered fcc phase, which at these lower temperatures develops bulk order slowly; growth is apparently too rapid to permit diffusive evolution of the stable L_{12} superstructure near the growth front. The disordered phase comprises hexagonal close packed sheets stacked in the three-layer repeat sequence ABCA... or ACBA... of the fcc lattice, given planes defined in figure 3(a). The two alternative structures so produced each have threefold rotational symmetry about [111], and are twins that transform one into the other by a mirror reflection (see below). The bcc reciprocal lattices of the two variants differ by this same reflection
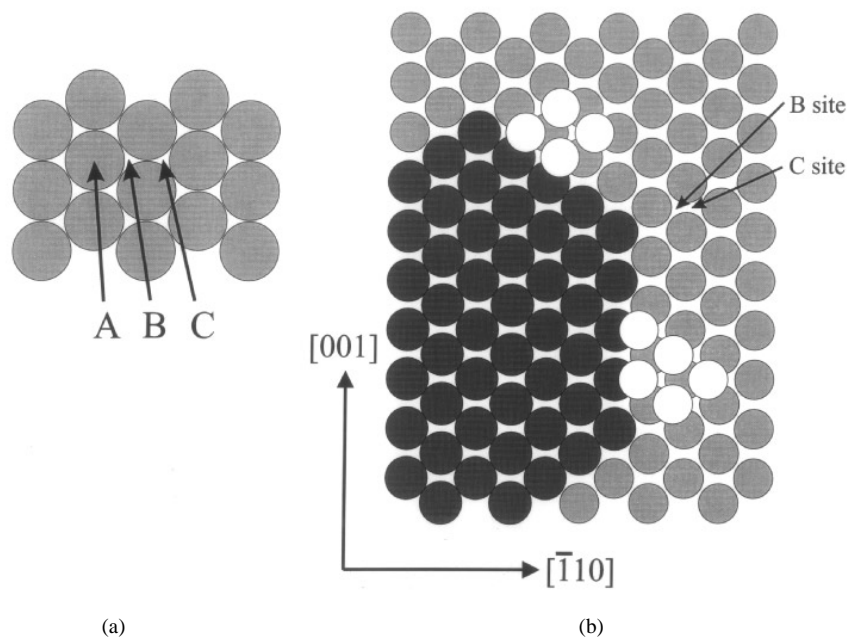
Figure 3. The ABC stacking of close packed planes that form the fcc lattice is shown at the left. At the right, the chemical effects of boundaries between fingered Nb (dark) and pseudomorphic first-layer Cu_3Au (grey) are traced. The open circles indicate preferred sites of the second layer. If the grey circles reconstruct into an fcc A plane, a subsequent B or C plane atom occupies one of the two available threefold hollow sites. The favoured second-layer sites shown reproduce the observed pattern of the template effect (see text).

and may therefore be distinguished from each other by x-ray diffraction. From the intensity ratio of the {220} reflections, our measurements determine the 'stacking ratio' as the relative volumes of the material with ABC and ACB stacking. The actual alloys used were allowed to order into L_{12} structures by aging, but this merely introduces additional superstructure reflections and does not alter the validity of the stacking analysis.

We have observed a remarkable variation of this stacking ratio, by a factor of $\sim$1000, which depends on the magnitude and direction of the miscut of the sapphire substrate. This is shown in figure 3 for miscuts up to about 1° in size. While the data are insufficient to reveal all details of the behaviour, the figure shows clearly that the ratio depends strongly on both the size and direction of the miscut. Only small biases occur for miscuts less than about 0.5°. However, ratios as large as 720 were observed for miscuts of $\sim$1° when a large component exists perpendicular to the bcc [001] direction. Thus, a selected miscut of $\sim$1° can cause the material to nucleate almost entirely in one of two equivalent structures. In order that figure 3 be most informative, each actual experiment has been plotted four times, using the global symmetry of the crystals to introduce each ratio in all four quadrants of the plane defined by [001] and [1̄10] axes in figure 3. It is worth emphasizing that the Cu_3Au crystals produced by the methods described here are of excellent quality, with (111) x-ray reflection linewidths of 0.07°, of which 0.04° can be attributed to the 3000 Å thickness of the film. The observed rocking curves are as low as 0.14°, which is due mainly to mosaic spread.

We now seek to explain the template effect by which the Nb surface selects a preferred
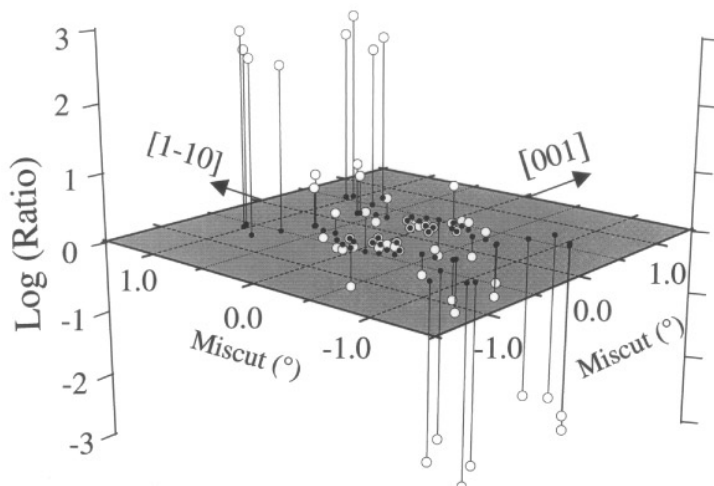
Figure 4. The logarithm of the observed stacking ratio (see text) shown as a function of miscut orientation and size and augmented using symmetry. While the available data do not define the behaviour completely, they do establish the strong directional dependence and large magnitude ($\sim 10^3$) of the template effect.

stacking. It is easy to see that this cannot be caused by the perfect (110) surface. Symmetry questions can readily be resolved when it is recognized: (a) that the two stacking sequences ABC and ACB (see figure 3(a)) are twins that are related by a mirror reflection in the plane perpendicular to the stacking displacements; and (b) that the epitaxial orientation of the Cu$_3$Au growth makes this twin plane parallel to the Nb(1$\bar{1}$0) plane. Because (1$\bar{1}$0) is a mirror plane of bcc Nb it is impossible from symmetry for the Nb(110) surface to distinguish between the two twins. We deduce that the observed stacking ratio must have its origin in departures from the perfect surface and more specifically in its vicinal miscut.

Further arguments of this type constrain the possible variations of the stacking ratio with Nb miscut. Positive and negative miscuts along [1$\bar{1}$0] produce Nb surface structures that are mutual mirror images in the (1$\bar{1}$0) plane, and these must therefore create mirror image epilayers. This means that the proportions of the two twins (which are mirror images in the (1$\bar{1}$0) plane) are thus interchanged. Again, since (001) is a mirror plane of Nb, the stacking ratio must remain unchanged when any component of miscut along [001] is reversed. In short, the logarithm of the stacking ratio must be an even function of the miscut along [001] and an odd function of the miscut along [1$\bar{1}$0]. This provides the basis for the data display presented in figure 4. The arguments neglect any possible effect of the underlying sapphire substrate on epitaxy, other than the vicinal miscut it transmits to the Nb buffer layer. Note that whichever sense along [1$\bar{1}$0] is chosen as positive, the preferred stacking appears as ABC because the two twins and the two senses of miscut along [1$\bar{1}$0] are both mirror images in (1$\bar{1}$0).

Some understanding of the effect of miscut on stacking may be acquired by considering a [001]-oriented Nb step caused by the miscut along [1$\bar{1}$0]. Such a step is shown by dark circles in figure 3(b), with the space below the step filled in by a pseudomorphic epilayer (grey circles). This is the direction of miscut that produces the strong effects of vicinal orientation in figure 4. It is normally observed in fcc epitaxy that a second noble metal layer starts the distortion of the initial pseudomorphic structure towards fcc [15]. We must

therefore ask how an underlying surface step can influence the way second-layer atoms (white circles in figure 3) occupy B or C sites, and thus nucleate a stacking selected for AB or AC. The B sites shown occupied at the [001] step in figure 3 are those that are found to be preferred in our experiments. In reality, the Nb mesostructures in figures 1 and 2 have (1$\bar{1}$0) facets that are not one but many [001] steps high. It is thus clear from the geometry that the closest C sites to these facets that are available for occupancy are further from the steps than the B sites shown occupied. If, as seems likely, a second-layer atom next to the step is attracted off the bridge site towards the (1$\bar{1}$0) facet and into the B site by the increased coordination it achieves, then this one process alone is sufficient to explain the sense of the stacking selection revealed by the experimental data collected in figure 4. A verification of this possible mechanism is a high priority for future calculations that address the energetics of heteroepitaxial stacking. Note that it is possible for the miscut along [001] to contribute additional terms to the dependence of stacking on surface orientation, but the present results do not identify any large contribution of this type.

In brief summary, we describe mesostructures that appear on the (110) surfaces of Nb about 500–1000 Å thick during epitaxial growth on sapphire (11$\bar{2}$0) at temperatures of 800–1000 °C. These are fingered structures that depend in a systematic way on the epilayer thickness, growth temperature and vicinal miscut of the substrate. In addition we report that these mesostructures create an important new template geometry at the Nb(110) surface. Specifically, the Nb exhibits a miscut dependent selectivity that discriminates between two equivalent twins that correspond to different stacking sequences for an fcc epilayer grown on this Nb template. This process offers practical use as a means of elimination stacking twins and hence improving structural coherence in heteroepitaxy. A microscopic mechanism for the selectivity is discussed in terms of (1$\bar{1}$0) facets caused by substrate miscut.

References

[1] Prinz G A 1985 *Phys. Rev. Lett.* **54** 1051
    Prinz G A *et al* 1986 *Appl. Phys. Lett.* **48** 1756
[2] Durbin S M, Cunningham J A and Flynn C P 1981 *J. Phys. F: Met. Phys.* **11** L223
    Cunningham J A, Durbin S M and Flynn C P 1982 *J. Phys. F: Met. Phys.* **12** L75
[3] McWhan D B 1985 *Layered Structures and Epitaxy (Mater. Res. Soc. Symp. 37)* ed J M Gibson and L R Dawson (Pittsburgh, PA: Materials Research Society)
[4] Cunningham J A and Flynn C P 1985 *J. Phys. F: Met. Phys.* **15** L221
[5] Huang J C A, Du R R and Flynn C P 1991 *Phys. Rev. Lett.* **66** 341
[6] Sonntag P, Donner W, Metoki N and Zabel H 1994 *Phys. Rev.* B **49** 2869
[7] Bonham S W and Flynn C P 1996 *Surf. Sci. Lett.* **366** L760
[8] Kwo J, Gyorgy E M, McWhan D, Hong M, DiSalvo F J, Vettier C and Bower J E 1985 *Phys. Rev. Lett.* **55** 1402
[9] Erwin R W, Rhyne J J, Salamon M B, Borchers J, Sinha S, Du R R and Flynn C P 1987 *Phys. Rev.* B **35** 6808
[10] Flynn C P and Yang M H 1996 *Mater. Res. Soc. Symp. Proc.* **401** 1
[11] Eaglesham D J and Cerullo M 1990 *Phys. Rev. Lett.* **64** 1943
[12] Mo Y-M, Savage D E, Swartzentruber B S and Lagally M G 1990 *Phys. Rev. Lett.* **65** 1020
[13] Tersoff J, Teichert C and Lagally M G 1996 *Phys. Rev. Lett.* **76** 1675
[14] Zhou G L and Flynn C P 1997 unpublished
[15] See e.g. Bauer E 1982 *Appl. Surf. Sci.* **11/12** 479
    Ruckman M W, Strongin M and Pan X 1987 *Mater. Res. Soc. Symp. Proc.* **83** 85